Loop-shaping Design with Constant Magnitude *Loci* in Control Education*

V. CERONE, M. CANALE and D. REGRUTO

Dipartimento di Automatica e Informatica, Politecnico di Torino, corso Duca degli Abruzzi, 24, 10129 Torino, Italy. E-mail: vito.cerone@polito.it

This educational contribution introduces the sensitivity peak beside the complementary sensitivity peak as indices of relative stability in the loop-shaping approach design of SISO control systems, through the use of an Extended Nichols Chart (ENC) which displays constant magnitude loci *of the sensitivity function along with the well-assessed constant magnitude* loci *of the complementary sensitivity. The advantages of using the ENC in an educational context will be shown in the control design of an unstable laboratory process.*

Keywords: control education; control system design; frequency-response methods; Nichols chart

INTRODUCTION

IN RECENT YEARS, the educational engineering community's attention has been drawn to the problem of improving automatic control teaching. Many contributions regarding different aspects of such a problem can be found in the recent Special Issue [1]. Here we describe a teaching project on analysis and design of feedback control systems for an undergraduate course in engineering curricula. Analysis and design of single-input, single-output control systems performed through basic Laplace transform techniques and employing standard frequency response tools like Bode, Nyquist and Nichols plots are the topics to be covered in the course (see the Appendix for a detailed description of the didactic organization of the course). In this context, a feedback cascade compensation scheme, as depicted in Fig. 1, is considered.

In such a structure, $G_p(s)$ and $G_c(s)$ are the plant and the controller transfer functions respectively. The bandwidth of the sensor is supposed to be wider than the bandwidth of the control system to be designed, hence in the working frequency range a static gain G_t can be used to describe the sensor behaviour. The static gain G_v is introduced in order to meet the desired input-output steady-state gain. The reference signal is r, y is the controlled output and u the control input. Additive output (d_y) and measurement (d_t) disturbances are also considered. The open loop system is denoted by $L(s) = G_c(s)G_p(s)G_tG_v$, the sensitivity function by $S(s) = 1/(1 + L(s))$ and the complementary sensitivity function by $T(s) = L(s)/(1 + L(s))$.

In the design procedures to be introduced in the given educational context, loop shaping techniques using standard PID, lag and lead controllers are employed. Thus, particular attention has to be

devoted to the relationships between the closed loop ($|T(j\omega)|$ and $|S(j\omega)|$) and the open loop ($L(j\omega)$) frequency responses, which are easily obtained on the Nyquist plane through the use of the constant magnitude loci M_T of $|T(j\omega)|$ (also referred to as the Hall chart, [2]) and constant magnitude *loci* M_S of $|S(j\omega)|$. While the former are part of standard methodologies for frequency domain analysis and design, the latter, to the best of the authors' knowledge, are not considered in classical textbooks for an undergraduate course on control system design. Some authors (see, e.g. [3], [4]), suggest that $|S(j\omega)|$ can be derived by drawing the frequency response of the inverse open loop transfer function $1/L(j\omega)$ and using the constant magnitude *loci* M_T of $|T(j\omega)|$. However, as it requires the drawings of two different plots at one time, this procedure may limit the effectiveness of such a tool in analysis and design. Besides, polar and/or Nyquist plots representations of the frequency response do not provide a direct reading of some properties of a given control system such as gain and phase margins. In fact, although both gain and phase margins are naturally defined on the Nyquist plane, they can be directly evaluated on the gain-phase plane through the intersections of the open loop plot with the vertical (−180°) and horizontal (0 dB) axes respectively. The gain-phase plane equipped with constant magnitude curves and constant phase curves of $T(j\omega)$ is the well-known Nichols chart. The first educational contribution of this paper, aimed at enhancing and simplifying the use of such an analysis and design tool, is to present an extended Nichols chart which displays constant magnitude *loci* M_S along with the well assessed constant magnitude *loci* M_T.

In order to show the effectiveness of the presented approach, and to boost its educational aspects, both computer simulated examples (using MatLab®) and laboratory practice on real
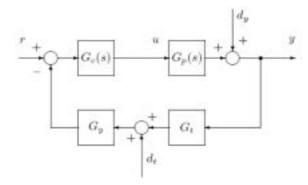
Fig. 1. The considered control structure.

processes are included in the course schedule (see Appendix). Laboratory experiments based on real systems are beyond all doubt appealing to students; they are challenging as well since they may show extra features which cannot arise in simulation, even if accurate models are considered. In fact, it is well known that model uncertainty, if not suitably taken into account, may lead to instability or, at the best, to poor performance of the control system. However, given the course context, robust analysis and design tools would be far behind the topics of the course, so suitable indices of stability and/or performance have to be effectively introduced. Indeed, classical control textbooks such as [4], [5], [6], remark on the need of taking into account both the gain and phase margins as measures of controlled system stability. However, both stability margins are considered explicitly only from the analysis point of view while the phase margin alone is usually considered in the design stage. A more general way to take care of phase and gain margins requirements is to consider both the maximum resonance peaks T_p and S_p of $|T(j\omega)|$ and $|S(j\omega)|$ respectively. The use of the M_T and M_S constant magnitude *loci* corresponding to T_p and S_p on the Nichols plane allows one to take into account such peak resonance requirements in the shaping of the open loop transfer function frequency response $L(j\omega)$. A number of papers have been published in recent years where M_T and/or M_S constant magnitude *loci* are used in the design of PID controllers (see, e.g. [7], [8], [9] and [10]).

While the peak T_p is a standard relative stability measure employed in basic control design, the value of S_p, though introduced in classical textbooks (see, e.g. [6]), is not considered in the design procedure. Indeed, since the quantity S_p can be easily related to the maximum plant perturbation that can be added before the closed loop system becomes unstable (see e.g. [11], [12]), a requirement on the sensitivity function resonance peak paves the way for the introduction of basic rudiments of robust control in such an undergraduate course. Note that further control design requirements such as low and high frequency disturbances attenuation can be handled by considering suitable constant magnitude loci on the Nichols plane. Summarising, the main educational contribution of the paper is the introduction of the peak S_p beside T_p, as indices of relative stability through the use of an extended Nichols chart in the loop-shaping approach design of SISO control systems.

PROBLEM FORMULATION

Consider the feedback control system of Fig. 1 above. The loop, sensitivity and complementary sensitivity transfer functions are defined, respectively, as

$$L(s) = G_c(s)G_p(s)G_tG_y \tag{1}$$

$$S(s) = \frac{1}{1 + L(s)} \tag{2}$$

$$T(s) = \frac{L(s)}{1 + L(s)} \tag{3}$$

The maximum sensitivity S_p and the maximum complementary sensitivity T_p are defined as

$$S_p = \max_{\omega \in [0,\infty]} |S(j\omega)| \tag{4}$$

$$T_p = \max_{\omega \in [0,\infty]} |T(j\omega)| \tag{5}$$

We shall go on to show how given upper bounds on Equations (4) and (5) can be employed in order to set out an effective guide to trial and error design in such a context. The steady-state design is deliberately skipped and it is assumed that requirements on steady-state polynomial reference tracking and/or polynomial disturbance attenuation/rejection are duly taken into account. It is well known that loop-shaping techniques are employed in the presence of frequency domain specification such as, e.g. sensitivity peak and complementary sensitivity peak requirements, low and/or high frequency disturbance attenuation, bandwidth, etc. As up-to-date instructors may know, frequency domain control systems design methods reported in classical undergraduate textbooks (see [3–6] and [13–24]) are based on phase margin (*PM*) and gain margin (*GM*) specifications, which, usually, are chosen on the basis of the designer's experience. In almost all the books in the lists of references, lower bounds on *PM* and *GM* are derived in terms of T_p, while only in a couple of textbooks (see e.g. [11], [24]), lower bounds on *PM* and *GM* are also derived in terms of S_p. In practice, however, only *PM* requirements are usually considered, while *GM* specs are almost entirely ignored and, unfortunately, even if conditions on *GM* and *PM* are fulfilled, satisfaction of desired given performance on T_p and S_p is not guaranteed. In this paper a frequency domain design approach based on loop shaping subject to the following constraints is presented

$$S_p \leq M_S^+ \qquad (6)$$

$$T_p \leq M_T^+ \qquad (7)$$

where $M_S^+ > 1$ and $M_T^+ > 1$ are upper bounds on sensitivity peak S_p and complementary sensitivity peak T_p respectively. Both S_p and T_p can be obtained from frequency domain specifications

on $S(j\omega)$ and $T(j\omega)$ which, for example, may have the shape shown in Fig. 2 and Fig. 3 respectively.

If frequency disturbance attenuation requirements are specified, further constraints can be added to the loop shaping problem. Indeed, if

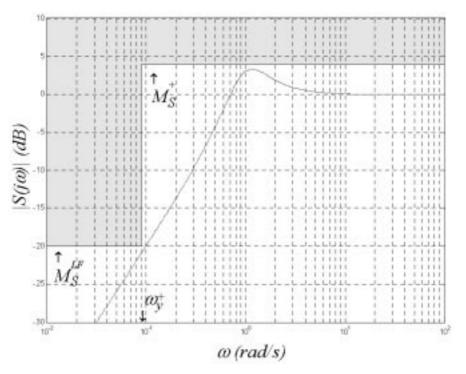$$d_y = a_y \sin \omega_y t \qquad \forall \omega_y \leq \omega_y^+ \qquad (8)$$

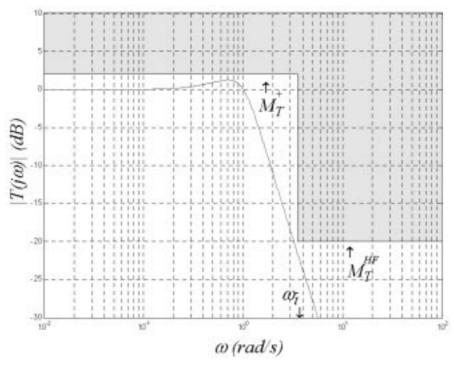Fig. 2. Frequency domain specifications on $|S(j\omega)|$.

Fig. 3. Frequency domain specifications on $|T(j\omega)|$.

where ω_y^+ and a_y are given, and the output error due to d_y is required to be bounded by a given ρ_y, then it is easy to see that the following constraint on $S(j\omega)$ can be derived:

$$|S(j\omega_y)| \leq \frac{\rho_y}{a_y} \doteq M_S^{LF} \qquad \forall \omega_y \leq \omega_y^+ \qquad (9)$$

where M_S^{LF} is the required low frequency attenuation level (see Fig. 2 above). While, if

$$d_t = a_t \sin \omega_t t \qquad \forall \omega_t \geq \omega_t^- \qquad (10)$$

where ω_t^-, and a_t are given, and the output error due to d_t is required to be bounded by a given ρ_t, then it is easy to see that the following constraint on $|T(j\omega)|$ applies:

$$|T(j\omega_t)| \leq \frac{\rho_t}{a_t} \doteq M_T^{HF} \qquad \forall \omega_t \geq \omega_t^- \qquad (11)$$

where M_T^{HF} is the required high frequency attenuation level (see Fig. 3 above).

As remarked in a couple of textbooks taken from the literature [6], [24], although PM and GM are considered as a classical measure of relative stability of nominal systems, they may fail to guarantee a reasonable bound on the distance of the loop transfer function $L(j\omega)$ from the critical point $(-1, 0)$ on the Nyquist plane. On the contrary, S_p, the maximum of $|S(j\omega)|$, can be successfully used to obtain simple bounds on both the phase margin and the gain margin. In other words, a single bound on S_p can be employed as a measure of robust stability in all closed loop stable systems, including the non-minimum phase and open-loop unstable cases in which both the PM and the GM are ill-defined. As a matter of fact, the maximum sensitivity S_p is the inverse of the shortest distance from the Nyquist plot of $L(j\omega)$ to the critical point $(-1, 0)$ on the complex plane, so it must be stressed that constraint Equation (6) can
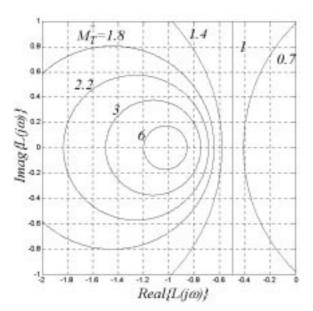
ensure stability robustness of the closed loop system subject to plant modelling uncertainty. Furthermore, although not so obvious, constraint Equation (7) provides robust stability as well when the plant is affected by multiplicative uncertainty [11]. Roughly speaking, the above ideas can be explained as follows: the presence of complex poles with small damping factor, i.e. poles near the $j-$axis, results in sharp and high peaks in both $|S(j\omega)|$ and $|T(j\omega)|$. Thus, constraining those peaks implies, in turn, forcing the closed loop poles suitably far from the imaginary axis.

It should be noted that the approach proposed in this work can be seen as a special case of the Quantitative Feedback Design Theory (QFT) which is an advanced methodology for dealing with plant uncertainty (see [25]). Indeed, given the plant templates, QFT converts closed-loop magnitude specifications (such as, e.g. (6), (7), (9), (11)) into magnitude and phase constraints on a nominal open-loop function. These constraints are called QFT bounds. However, Horowitz's approach is much too advanced to be introduced to undergraduate students.

THE NICHOLS CHART REVISITED AND EXTENDED

If $L(j\omega) = X + jY$, it is well known that the *loci* of constant $|T(j\omega)| = M_T$ in the Nyquist plane are the circles given by

$$Y^2 + \left(X + \frac{M_T^2}{M_T^2 - 1}\right)^2 = \frac{M_T^2}{(M_T^2 - 1)^2} \qquad (12)$$

when $M_T \neq 1$. If $M_T = 1$, it can be shown that the *loci* are described by $X = -\frac{1}{2}$, which is a straight line parallel to the Y axis and passing through the point $(-\frac{1}{2}, 0)$. Equation (12) represents a circle
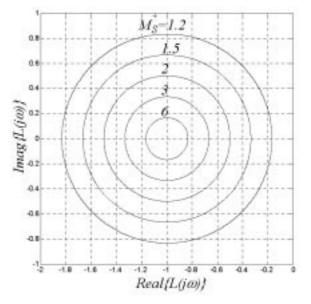

Fig. 4. M_T-circles on the Nyquist plane.

Fig. 5. M_S-circles on the Nyquist plane.

of radius $M_T/|(M_T^2 - 1)|$ centred on the real axis $(Y = 0)$ at $X = -M_T^2/(M_T^2 - 1)$, which are also called M_T−circles, whose use both for analysis and design is well known. Figure 4 shows some of the constant-$|T|$ circles. To the best knowledge of the authors, the locus of points corresponding to constant-$|S|$ is not considered in any of the undergraduate textbooks in the list of references. It is a bit less involved of the constant-$|T|$ circles and is a circle given by

$$Y^2 + (X + 1)^2 = \frac{1}{M_S^2} \tag{13}$$

Figure 5 shows some of the constant-$|S|$ circles, which are here referred to as M_S−circles. Constant-$|S|$ circles can be successfully employed for analysis and design in the same way as constant-$|T|$ circles. It is emphasized that setting upper bounds on T_p and S_p is equivalent to drawing a couple of 'forbidden' circles, around the critical point $(-1, 0)$, inside which $L(j\omega)$ is not allowed to lie (see, e.g. Fig. 6 below). Constant magnitude and/or phase circles are easily understood in the complex plane where polar and Nyquist plots are usually drawn.

However, constant magnitude contours can also be plotted on the gain-phase plane which displays the gain (in decibels) versus the phase (in degrees) readily available from Bode plots. A major disadvantage in working in the polar coordinates plane with the Nyquist plot of $L(j\omega)$ is that the curve no longer retains its original shape when simple modifications on the loop gain are made. Indeed, when design changes are required to meet a set of given specifications, it is often necessary to develop additional insight into cause and effect relationships. One approach is to use the gain-phase plane which often makes it possible a straightforward assessment of the changes that are required to

satisfy design specifications. For example, when the static loop gain is modified, the $L(j\omega)$ curve is shifted upwards or downwards in the vertical direction without distortion. From a Nichols chart and a gain-phase plot of $L(j\omega)$, we can read, for any frequency point, the magnitude and phase of $T(j\omega)$. In particular, we can easily evaluate the peak value of $|T(j\omega)|$. In some textbooks, see e.g. [4], it is suggested that the Bode plot of $|S(j\omega)|$ can be derived from the Nichols chart by plotting the *locus* of $L^{-1}(j\omega)$ rather than $L(j\omega)$ and using constant-$|T|$ curves. However, in the authors' experience, that procedure is rather too involved since we must draw both the direct and the inverse plot of $L(j\omega)$. Instead, we propose using constant-$|S|$ curves beside well-known constant-$|T|$ curves on the gain-phase plane, which will be referred to the *Extended Nichols Chart* (*ENC*). It is suggested that use of the *ENC* with (a) one constant-$|T|$ curve with level M_T^+, (b) one constant-$|S|$ curve with level M_S^+, (c) one constant-$|T|$ curve with level M_T^{HF} which takes into account a possible requirement on high frequency disturbance attenuation (if any) and (d) one constant-$|S|$ curve with level M_S^{LF} which takes into account a possible requirement on low frequency disturbance attenuation (if any). Figure 7 below shows a possibile *ENC* with $M_T^+ = 1.23$, $M_S^+ = 1.54$, $M_T^{HF} = 0.1$ and $M_S^{LF} = 0.1$.

CONTROLLER DESIGN FOR A REAL LABORATORY PROCESS USING THE ENC

The main purpose here is to highlight that the *ENC* allows students to design robust and effective controllers for a real plant by means of basic loop shaping techniques. As is well known (see, e.g. [26],
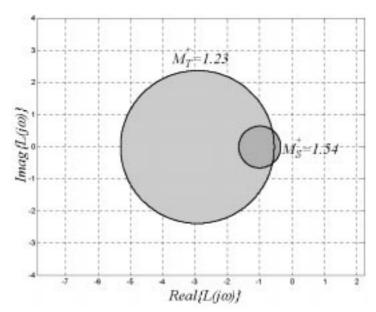

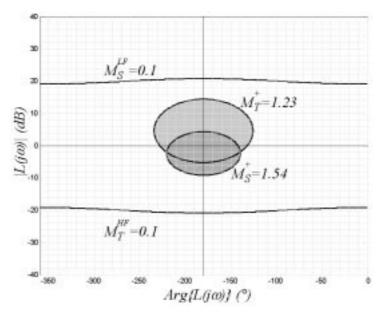Fig. 6. Nyquist plane with M_T-contours and M_S-contours.

Fig. 7. Extended Nichols Chart with M_T and M_S contours.

[27], [28]) the magnetic levitation system is inherently non-linear and unstable; the control of such a system is not a trivial task, especially for inexperienced undergraduate students. The levitation system shown in Fig. 8 below, is equipped with an optical sensor which converts the ball position into a voltage signal and with a transconductance amplifier which converts the voltage command computed by the controller into the current flowing through the electromagnet coil. For a detailed description of the considered levitation system the reader is referred to the book [29] and the Internet Web page *www.ladispe.polito.it/it/html/levitatore.htm*. A standard Intel® Celeron® 500 computer equipped with the MatLab® Real Time Workshop® is used for the implementation of the controller with a sampling time $T_s = 0.001$ s.
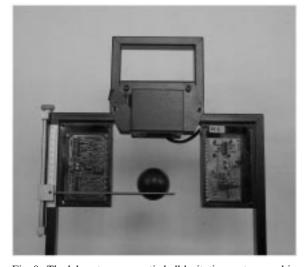

Fig. 8. The laboratory magnetic ball levitation system used in the example.

The following approximated linear model of the system has been obtained through linearization around a suitable operating point (u^o, y^o):

$$G_p(s) = \frac{-15.34}{(s - 30.34)(s + 30.34)} \qquad (14)$$

$$G_t = 555.89 \; V/m \qquad (15)$$

where, with reference to the block diagram of Fig. 1 above, $G_p(s)$ is the transfer function from the voltage command $u(t)$ to the the ball position $y(t)$, G_t is the static gain describing the optical transducer and $G_y = 1$ which implies that the input-output static gain equals $1/G_t$. The students are required to design a digital filter in order to control the position of the suspended ball around the operating point. More precisely, the closed loop system has to satisfy the following tracking performance specifications when the reference signal $r(t)$ is a zero-mean valued square wave with period $T_r = 4$s, duty cycle 50% and amplitude $r_a = 0.1$ V which corresponds to a ball displacement of about 0.18 mm around the operating point:

- (S1) zero steady-state error for a step reference;
- (S2) rise time $t_r \leq 0.015$ s;
- (S3) overshoot $\hat{s} \leq 25\%$.

In order to exploit frequency domain techniques for the controller design, time domain specifications (S1)—(S3) have to be converted into suitable frequency domain constraints. As is well known, specification (S1) simply requires an integrator in the controller in order to get a type I control system. As far as specifications (S2) and (S3) are concerned, relations between time domain and frequency domain response of prototype second-order systems can be exploited to get the following
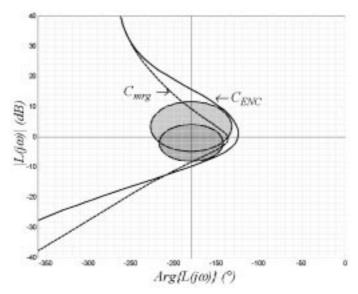
Fig. 9. Ball levitation system loop transfer function plot on the ENC: C_{ENC} (solid) and C_{mrg} (dashed).

bounds on the cross-over frequency ω_c and the closed loop peaks T_p and S_p:

$$\omega_c > \omega_c^- = 120 \ rad/s \qquad (16)$$

$$T_p < M_T^+ = 1.35 \ (2.6 \ dB) \qquad (17)$$

$$S_p < M_S^+ = 1.65 \ (4.35 \ dB) \qquad (18)$$

The *ENC* with $M_T^+ = 1.35$ and $M_S^+ = 1.65$ is shown in Fig. 9. The following controller with three lead networks has been designed to satisfy inequality (16) and the constraints on the *ENC* defined by the constant-$|T|$ curve with level M_T^+ and the constant-$|S|$ curve with level M_S^+:

$$C_{ENC}(s) = \frac{-19(s/30 + 1)^2(s/400 + 1)}{s(s/3200 + 1)(s/900 + 1)^2} \qquad (19)$$

The digital loop transfer function $L_{ENC}(z)$, provides a cross-over frequency $\omega_c \approx 209$ rad/s and satisfies the constraints on the *ENC* as shown in Fig. 9.

In order to show the educational benefits of the use of the *ENC*, $C_{ENC}(s)$ is compared with a controller designed exploiting the classical approach based on gain and phase margins specifications. To this end the following relations (see e.g. [24], [11]) can be used to obtain lower bounds on the gain and phase margins from Equations (17) and (18): $GM > GM^+$ and $PM > PM^+$, where

$$GM^+ = \max\left\{\frac{S_p}{S_p - 1}, \ 1 + \frac{1}{T_p}\right\} \approx 2.54 \ (8 \ dB) \qquad (20)$$

$$PM^+ = \max\left\{2\arcsin\frac{1}{2S_p}, \ 2\arcsin\frac{1}{2T_p}\right\} \approx 43.5^o. \qquad (21)$$

The following controller with three lead networks has been designed to satisfy the constraints $\omega_c > \omega_c^-$, $GM > GM^+$ and $PM > PM^+$:

$$C_{mrg}(s) = \frac{-40(s/75 + 1)^3}{s(s/525 + 1)^3} \qquad (22)$$

The digital loop transfer function $L_{mrg}(z)$, provides a cross-over frequency $\omega_c \approx 155$ rad/s, a gain margin $GM \simeq 8.3$ dB and a phase margin $PM \simeq 44^o$ as shown in Fig. 9 above.

The frequency responses of the complementary sensitivity and the sensitivity functions obtained with the controllers C_{ENC} and C_{mrg} and computed on the basis of the approximated linear model $G_p(s)$ are shown in Fig. 10. As expected, the closed loop control system obtained with the controller C_{ENC} satisfies the frequency domain performance specifications on the peaks of $|S(j\omega)|$ and $|T(j\omega)|$ while that is not the case for the closed loop system obtained with the controller C_{mrg}.

The experimental square wave responses obtained with the controllers C_{ENC} and C_{mrg} are shown in Fig. 11 below. Neither closed loop system satisfies the performance specification (S3) on the overshoot; that is due to (i) the fact that the relations used to map time domain specification (S1)—(S3) into the frequency domain constraints Equations (16), (17) and (18) are exact only for prototype second-order systems while the obtained closed loop system is not and (ii) the effect of the mismatch between the approximated linear model used for the design of the controllers and the complex non-linear dynamics of the real plant. However, it can be noted that, in spite of (i) and (ii), the controller designed on the basis of the *ENC* guarantees a maximum overshoot $\hat{s} \approx 31\%$; on the contrary the response of the closed loop systems obtained with the controller C_{mrg} shows lightly damped oscillations and a maximum overshoot $\hat{s} = 105\%$.
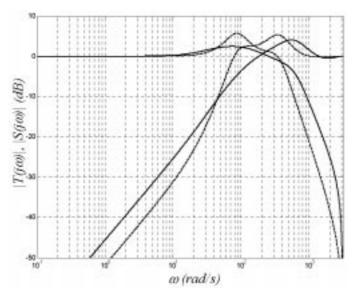
Fig. 10. Ball levitation system frequency response with: C_{ENC} (solid) and C_{mrg} (dashed).
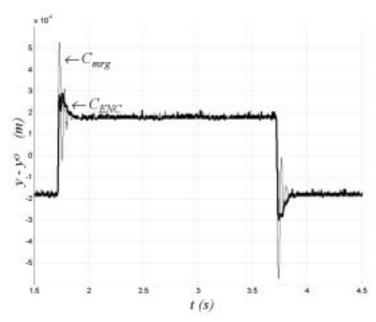

Fig. 11. Ball levitation system experimental square wave response with C_{ENC} (thick) and C_{mrg} (thin).

DISCUSSION

In the example above, the performance of two controllers on a real plant were compared: the first controller, C_{ENC}, was designed using the proposed *ENC* equipped with constant-$|T|$ curve with given level M_T^+ and the constant-$|S|$ curve with given level M_S^+; while the second one, C_{mrg}, was designed on the ground of gain and phase margin constraints. The aim of the example is twofold. First, the classical frequency domain design approach, based on gain and phase margin requirements, can lead to closed-loop systems which do not satisfy typical frequency domain performance specifications on $|S(j\omega)|$ and $|T(j\omega)|$ of the kind shown in Fig. 2 and Fig. 3

above; also, such a design method may also fail to guarantee good robustness. Second, it has been shown that the *ENC* is a simple and effective tool to fulfil performance specifications expressed in terms of constraints on the frequency response of S and T. Trying to avoid the 'forbidden region' delimited by the constant-$|T|$ curve with given level M_T^+ and the constant-$|S|$ curve with given level M_S^+, the student is guided through the design of an inherently robust control system.

CONCLUSION

An extended Nichols chart which displays constant magnitude *loci* of both complementary

sensitivity and sensitivity functions has been proposed as an effective tool for analysis and design of feedback control systems. It has been shown that, through the use of such a chart, stability indices such as resonance peaks of both complementary sensitivity and sensitivity functions can be easily handled, providing much more insight and guiding hints than gain and phase margins for the sequence of the loop-shaping design trials. Thanks to the ENC, loop-shaping control design can be effectively performed by a skilled designer and inexperienced students, since both will take advantage from the pair of constant magnitude curves which provide a couple of forbidden regions inside which the open-loop transfer function frequency response is not allowed to lie. The use of the ENC for the control design of an unstable laboratory process has been included in order to show its effectiveness in automatic control education.

REFERENCES

1. International Journal of Engineering Education, *Special Issue on Innovative Approaches to Control Engineering Education,* **21**(6), 2005.
2. A. Hall, *The analysis and synthesis of linear servomechanisms*. Cambridge, MA: Technology Press, M.I.T., (1943).
3. J. D'Azzo and C. H. Houpis, *Linear control system analysis and design: conventional and modern*, 4th ed. New York: McGraw–Hill, (1995).
4. B. J. Kuo and F. Golnaraghi, *Automatic Control Systems*, 8th ed. New York: John Wiley & Sons (2003).
5. R. C. Dorf and R. H. Bishop, *Modern Control Systems*, 10th ed. Upper Saddle River, New Jersey, Prentice-Hall, (2004).
6. G. F. Franklin, J. D. Powell and A. Emami-Naeini, *Feedback Control of Dynamic Systems*, 4th ed. New Jersey, Macmillan Publishing Company, (2002).
7. K. Astrom and T. Hagglund, *Advanced PID Control*, Research Triangle Park, NC 27709 ISA—The Instrumentation, Systems, and Automation Society, (2006).
8. K. Astrom, H. Palagopuos and T. Hagglund, Design of PI controller based on non-convex optimization, *Automatica*, **34**(5) 1998, pp. 585–601.
9. B. Kristiansson and B. Lennartson, Robust and optimal tuning of PI and PID controllers, *IEE Proc. Control Theory Appl.*, **149**(1), 2002, pp. 17–25.
10. O. Yaniv and M. Nagurka, Design of PID controllers satisfying gain margin and sensitivity constraints on a set of plants, *Automatica*, **40,** 2004, pp. 111–116.
11. S. Skogestad and I. Postlethwaite, *Multivariable Feedback Control*, 1st ed. New York, John Wiley & Sons, (1996).
12. J. C. Doyle, B. A. Francis and A. R. Tannenbaum, *Feedback Control Theory* New York, Macmillan Publishing Company, (1992).
13. R. T. Stefani, B. Shahian, C. J. Savant Jr. and G. H. Hostetter, *Design of Feedback Control Systems*, 4th ed. New York: Oxford University Press, (2002).
14. C. T. Chen, *Control System Design*. Orlando, Florida, Saunders College Publishing, (1993).
15. J. J. Di Stefano, A. R. Stubberud and I. J. Williams, *Feedback and Control Systems*, 2nd ed. New York, McGrawHill, (1990).
16. G. Dutton, S. Thompson and B. Barraclough, *The Art of Control Engineering*. Addison Wesley Longman, (1997).
17. G. C. Goodwin, S. F. Graebe and M. E. Salgado, *Control System Design*. Upper Saddle River, New Jersey, Prentice-Hall, (2001).
18. P. H. Lewis and C. Yang, *Basic Control Systems Engineering*. Upper Saddle River, New Jersey, Prentice-Hall, (1997).
19. N. S. Nise, *Control Systems Engineering*, 4th ed. New York, John Wiley & Sons, (2004).
20. K. Ogata, *Modern Control Engineering*, 3rd ed. Upper Saddle River, New Jersey, Prentice-Hall, (1997).
21. C. L. Phillips and R. D. Harbor, *Feedback Control of Dynamic Systems*, 4th ed. Upper Saddle River, New Jersey, Prentice-Hall, (2000).
22. C. E. Rohrs, J. L. Melsa and D. G. Schultz, *Linear Control Systems*. New York, McGraw-Hill, (1993).
23. J. Van de Vegte, *Feedback Control Systems*, 3rd ed. Englewood Cliffs, New Jersey, Prentice-Hall, (1994).
24. W. A. Wolovich, *Automatic Control*. Orlando, Florida, Saunders College Publishing, (1994).
25. I. Horowitz, *Quantitative feedback theory*. Boulder, Colorado, QFT Publications, (1993).
26. V. A. Oliveira and E. F. Costa, Digital implementation of magnetic suspension control system for laboratory experiments, *IEEE Trans. Educ.* **42**(4), 1999, pp. 315–322.
27. P. S. Shiakolas and D. Piyabongkarn, Development of a real-time digital control system with hardware-in-the-loop magnetic levitation device for reinforcement of controls education, *IEEE Trans. Educ.*, **46**(1), pp. 79–87, 2003.
28. R. K. H. Galväo, T. Yoneyama, F. M. U. de Araújo, and R. G. Machado, A simple technique for identifying a linearized model for a didactic magnetic levitation system, *IEEE Trans. Educ.* **46**(1), 2003, pp. 22–25.
29. C. Greco, M. Rulla, and L. Spagnolo, *Laboratorio sperimentale di automatica.*, Milano, Italy, McGraw-Hill Italia, (2003).

APPENDIX

This section provides some details about the course scope, its structure and organization.

Required background: basic mathematics and physics courses commonly provided in the first two years of the italian engineering curricula.

Course topics: analysis and design of single-input, single-output control systems performed through basic Laplace transform techniques and employing standard frequency response tools like Bode, Nyquist and Nichols plots.

Course organization: the didactic activity is organized as follows:

- *Course term.* seven weeks.
- *Lectures* (six hours/week). The teacher (a faculty member) introduces the methodological facts and present a number of suitable numerical examples.
- *Computer aided laboratory* (2 hours/week). The students are required to solve a set of suggested problems using MATLAB and/or Simulink software packages. During this activity students work alone. The teacher assists the students with the help of a teaching assistant (usually a Ph.D student). Some of the assignment are introductory to the experimental laboratory activities. In particular, students have to perform the control design and the related simulation tests needed before the laboratory implementation.
- *Experimental laboratory* (4 hours in total). In the first two hours, the students are required to collect the experimental data needed to derive a suitable mathematical model of the laboratory process (DC motor, magnetic levitation system, inverted pendulum, etc.). In the last two hours, they have to implement the controller previously designed during the Computer aided laboratory. Collection of closed-loop experimental data is required to verify the achievement of the assigned specifications. During these activities students work in small groups (three or four people).

Vito Cerone received the Laurea degree in Electronic Engineering in 1984 and the Ph.D. degree in System Engineering in 1989, both from the Politecnico di Torino. He is an Associate Professor at the Politecnico di Torino where he teaches Analysis of Dynamic Systems, Feedback Control System Design, Analysis and Design of Physiological Systems. His main research interests are in system identification, parameter estimation, control, optimization and their applications.

Massimo Canale received the Laurea degree in Electronic Engineering (1992) and the Ph.D. degree in System Engineering (1997), both from the Politecnico di Torino, Italy. From 1997 to 1998, he worked as a software engineer in the R&D department of Comau Robotics, Italy. Since 1998, he has been an Assistant Professor in the Dipartimento di Automatica e Informatica of the Politecnico di Torino where he teaches System Theory and Automatic Control. His research interests include robust control, model predictive control, set membership approximation and application to automotive and aerospace problems.

Diego Regruto received the Laurea degree in electronic engineering and the Dottorato di ricerca degree in System Engineering, both from Politecnico di Torino in 2000 and 2004 respectively. He is currently an Assistant Professor at the Dipartimento di Automatica e Informatica, Politecnico di Torino. His main research interests are in the fields of system identification and robust control, with application to automotive problems.